Chapter 4

Vortex Generation, Experimental Characterization, and Application in Turbulent Flows

Guillermo Martin Capittini,
Julio Marañon Di Leo and Juan Sebastian Delnero

Additional information is available at the end of the chapter

http://dx.doi.org/10.5772/intechopen.79504

Abstract

This chapter is focused on vortex detection, generation, and characterization. There are many ways to generate and characterize vortex; this chapter is focused on two techniques to generate a vortex, with fixed surface, often called vortex generators (VG), and with blowing air. Vortex detection is one of the major problems in fluid dynamics and usually some characteristics of the vortex must be known in order to detect them; once, the vortex is detected, a velocity analysis is helpful to characterize it. Most characterization techniques involves the comparison of some known properties of vortex, such as velocity field, vorticity field or tensor, turbulence intensity, etc. The technique to be used to characterize a vortex is closely related to the data that one possesses. In measuring methods such as particle image velocimetry (PIV), there are algorithms that can easily detect size and vortex centers, relaying in velocity and vorticity. This chapter focuses on detection by analyzing velocity signals, via wavelet transform and statistical properties. When it is not possible to characterize a vortex because it does not have a coherent structure, another approach must be used such as defining turbulence intensities and zone of influence of the vorticose structure.

Keywords: vortex, detection, characterization, turbulence, generation

1. Introduction

Determining exactly how a system is going to behave in aerodynamics can be a challenge. This is because the incident flow plays a main role in the behavior. A wing immersed in a turbulent flow is not going to experiment the same forces as it would in a laminar flow. Even a change in the turbulent scales can conduct to a variation in the aerodynamic coefficients of the wing. This phenomenon can become much critic for large vortex, where even the relative position of the vortex over the wing is going to play a role in the wing efficiency.

For decades, this reason has led scientist and engineers to study systems' behavior in different conditions of the free flow. To do this, one must be able to change the flow conditions in terms of turbulence and turbulent scales, here is where different kinds of vortex and turbulent generators came along. There is a wide variety of techniques to create vortexes; an usual and widely used is Von Karman streets as in [1], or delta wing VG as in [2–4]. These methods involve fixed surfaces, but there are others where energy and mass are injected in the flow, to create the vorticose structure. Once, the vortex is created, a full characterization must be performed to determine the flow condition. In modern measurement techniques such as particle image velocimetry (PIV), very effective algorithms can be used to characterize the flow, such as [5], but for anemometric measurement, this can represent quite a challenge.

This chapter's intention is to give a good introduction to vortex identification techniques, as well as the characterization and the generation, and in the ending showing results of how the presence of different vorticose flow configurations can lead to a modification in a system behavior.

2. Characterization

There are different ways to characterize a vortex. As told before, this chapter covers the characterization of vortex measured with anemometers. The idea here is to find if there is a vortex passing by analyzing the evolution of velocity over time in a given point or in set of points. This section mainly focuses in the use of continuous wavelets transform to identify a vortex immersed in a turbulent flow.

Let us consider for porpoise of demonstration a simulated signal. To do so, lets define the velocity distribution of a 2D vortex. There are many kinds of vortex, rotational and irrational, physically plausible and not, and for this example and for the purpose of demonstration, a Rankine vortex is going to be used. This kind of vortex is an approximation of a real one, since it does not take into account the effect of the fluid viscosity. Due to the neglect of viscosity, these kinds of vortexes do not vanish over time. Another more general one is a Lamb-Oseen vortex, this is an exact solution to the Navier–Stokes equations, and it does take into account the effect of viscosity. But for the purpose of this simulation, there is no need to use it.

A Rankine vortex has a velocity distribution as shown in Eq. (1) as shown in [6].

$$V_\theta(r) = \begin{cases} \dfrac{\Gamma r}{2\pi R^2} r < R \\ \dfrac{\Gamma}{2\pi r} r < R \end{cases} \tag{1}$$

It is seen in this distribution that the flow velocity increases linearly until it reaches a radius R and then decreases like 1/r as shown in **Figure 1**.

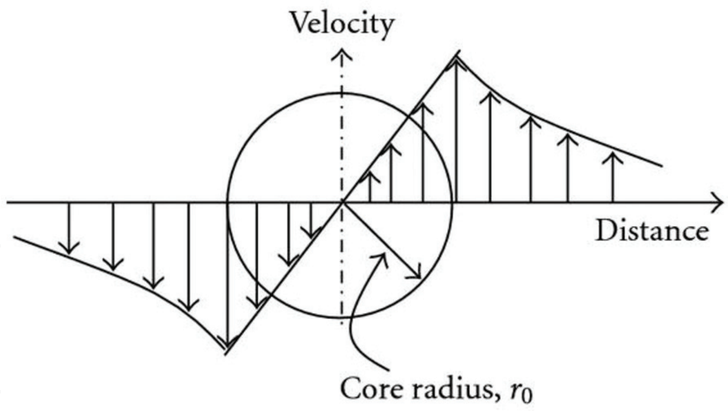

Figure 1. Velocity distribution on a Rankine vortex.

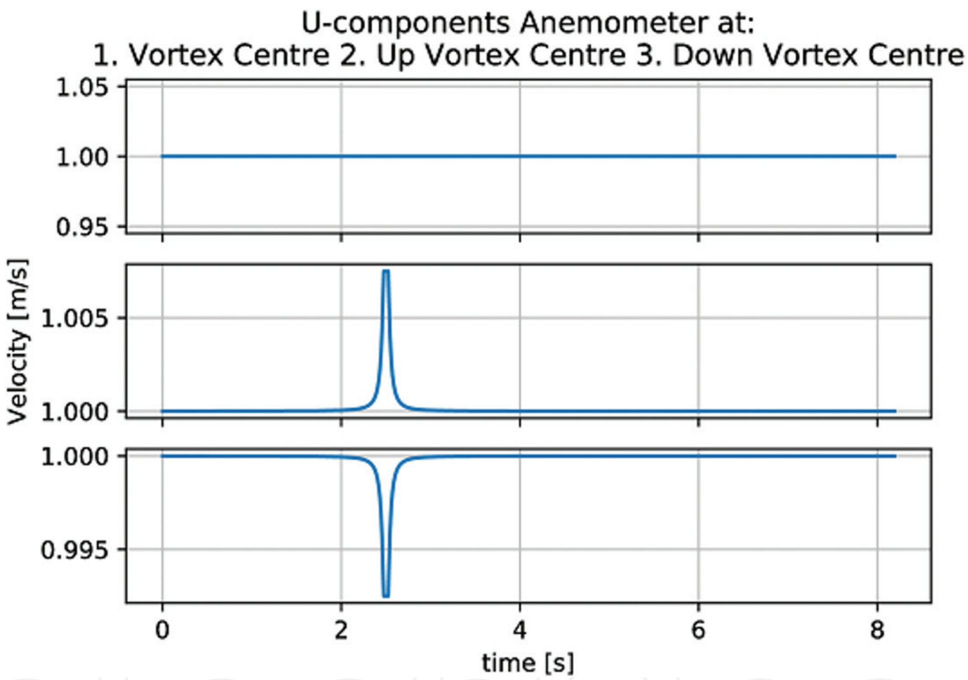

Figure 2. Velocity distribution on a Rankine vortex U-component.

Now, if a single vortex is moving with flow velocity, and an arrangement of anemometers is settled to capture the U-component (flow direction) and V-component (perpendicular to flow direction), in case the anemometer captures the vortex, there are three possibilities, to capture it exactly on its center, up, or down to it. **Figures 2** and **3** show the signals that would be obtained in such cases.

As it is shown, the V-component signal shape does not change substantially, but the U-component, clearly evidence if the vortex is over or under the anemometer, for a clockwise vortex, it would be opposite for a counterclockwise. Because of the velocity distribution of a vortex, the U-component is not going to evidence by itself the passage over an anemometer.

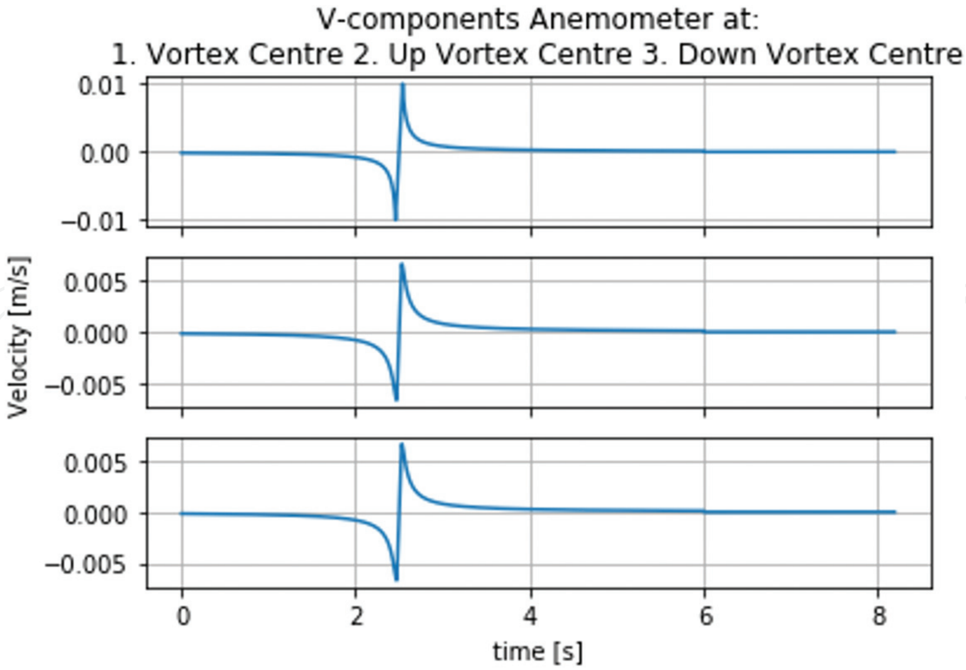

Figure 3. Velocity distribution on a Rankine vortex V-component.

Watching the V-component, one can clearly distinguish that a vortex has passed through the anemometer, by the change in the velocity sign.

This simplified case shows our goal, that is, to determine if this kind of structure is present in a velocity signal.

In these simple cases, a vortex passage is easy to identify, but in the presence of a highly turbulent flow, this task is not so trivial, and more advance techniques or experimental setups are required.

For simplicity, from now on, only an anemometer above the vortex center is going to be considered. It must be said that in an experimental setup, one usually do not know where exactly the vortex center is going to be, so multiple measurements must be taken until this position is determined. In a steady flow, a coherent structure becomes periodic, so the passage would repeat over a time t_p, and a signal similar to the one shown in **Figure 4** is expected.

Given this type of signal, a useful tool in vortex detection can be introduced, that is, the continuous wavelet transform (cwt). The cwt is useful to find coherent structures of a certain shape inside a signal, for more information of detection using wavelet transform, see [7–9]. To detect these structures, there are two useful wavelets: the derivative of Gaussian function of order 1 (DOG1) and the one of order 2 (DOG2) (also known as the Ricker wavelet). Both wavelets are plotted in **Figure 5**. Using DOG1 for the V-component and DOG2 for the U-component, one is able to detect a vortex passage.

It is seen in **Figures 6** and **7** that every time a vortex goes through the anemometer, a maximum of the wavelets coefficient occurs.

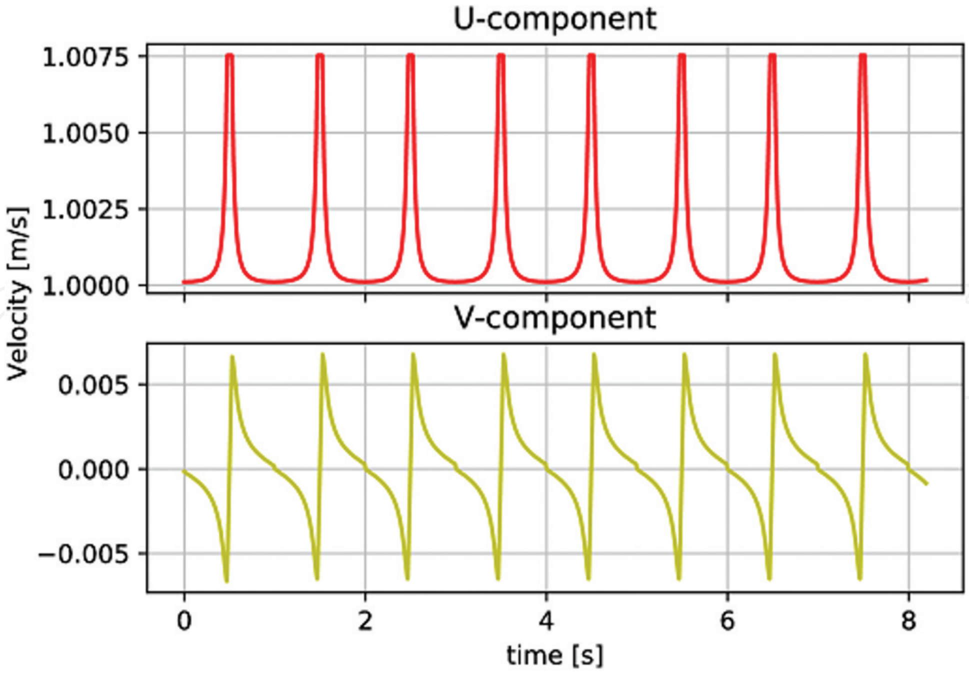

Figure 4. Velocity signal for a periodic vortex.

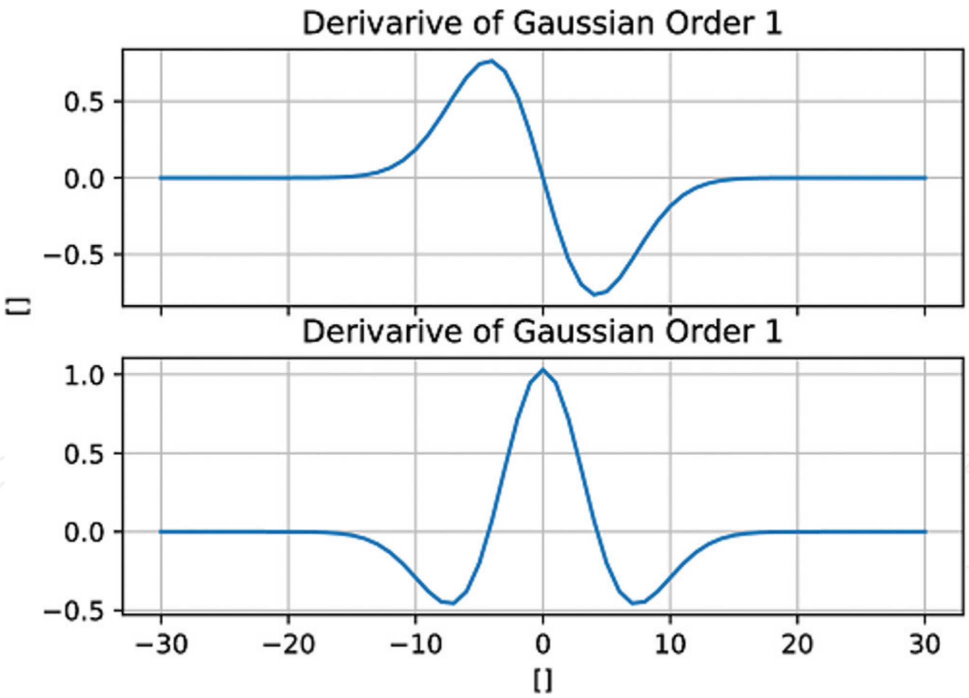

Figure 5. Wavelets used for detection.

This may seem trivial since one can easily detect the vortex passage in the velocity signals. But when turbulence is present in the free flow, it becomes harder to determine if and when a vortex is passing.

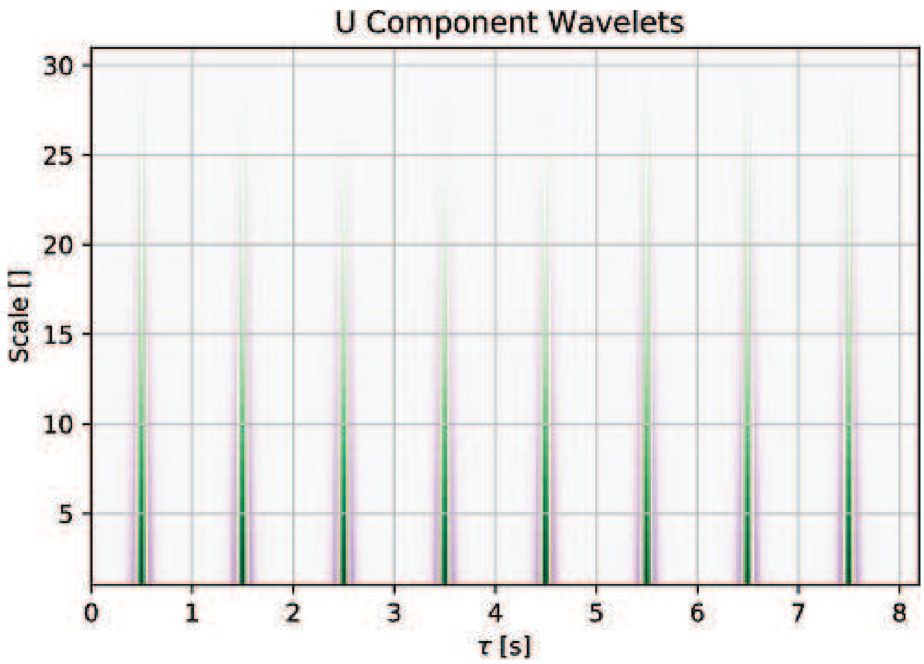

Figure 6. Wavelets coefficients in U-component.

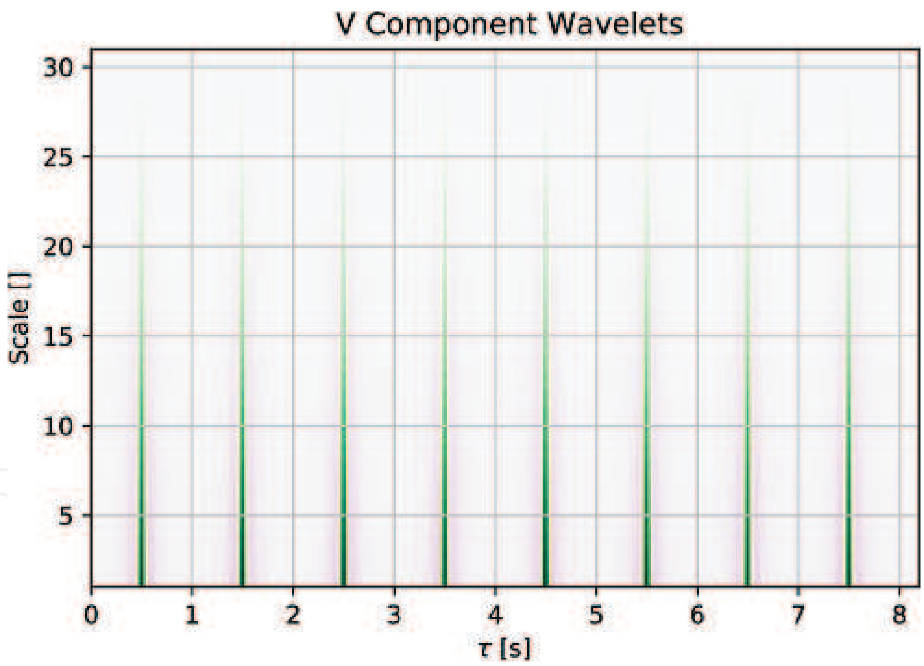

Figure 7. Wavelets coefficients in V-component.

To consider the mentioned problem, from now on, a turbulent flow is going to be treated. For this purpose, a random signal is added to our periodic vortex. This signal is going to simulate turbulence, and it is going to be generated by a random noise with a Gaussian distribution. It must be said that this is for demonstration purposes only, since a random noise does not fully represents a turbulent flow, and does not fulfill the constrains imposed by the "Kolmogorov – 5/3 spectrum."

http://dx.doi.org/10.5772/intechopen.79504

But the techniques presented here, give similar results for these simulated signals with Gaussian noise and for measured signals with real turbulence.

Let us first define the so-called turbulence intensity. This property is useful to characterize a turbulent flow, since the vortex present in it is usually noncoherent, this property gives us, not the velocity function, but a measure of how much energy is present in the turbulence. And it is defined as in Eq. (2)

$$T_i = \frac{\sigma_u}{\mu_u} \tag{2}$$

where σ_u represents the standard deviation of the velocity component, and μ_u the mean value of the same component.

For this simulation, a turbulence intensity of 2% is going to be set; this is a normal value for wind tunnel testing and the maximum value of the vortex tangential velocity is going to be 3% of the flow mean velocity, and with a characteristic radius of 4 cm. **Figures 8** and **9** shows both components of velocity and a wavelet map for the V-Component.

It can be seen that when turbulence is present in the free flow, a vortex passage is not easily found. But **Figure 9** shows that analyzing the wavelet coefficients of the DOG1 in the V-component, the passage becomes obvious. This becomes a powerful tool, since it allows one to detect a vortex passage even when the turbulent velocity fluctuation is in the order of the maximum vortex velocity.

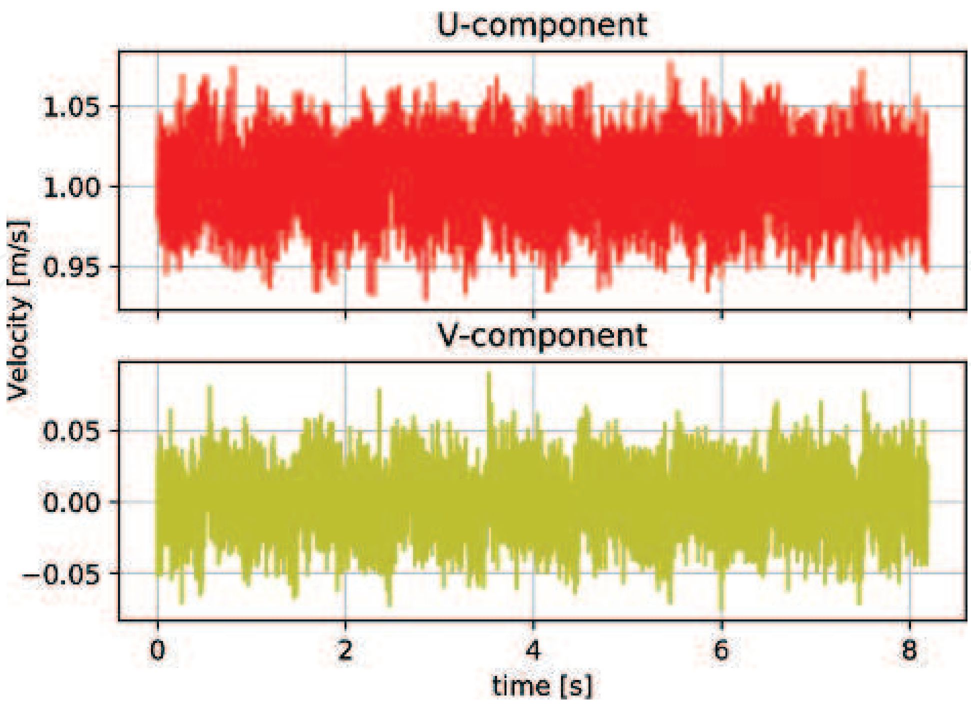

Figure 8. Velocity signals for a periodic passage with turbulence.

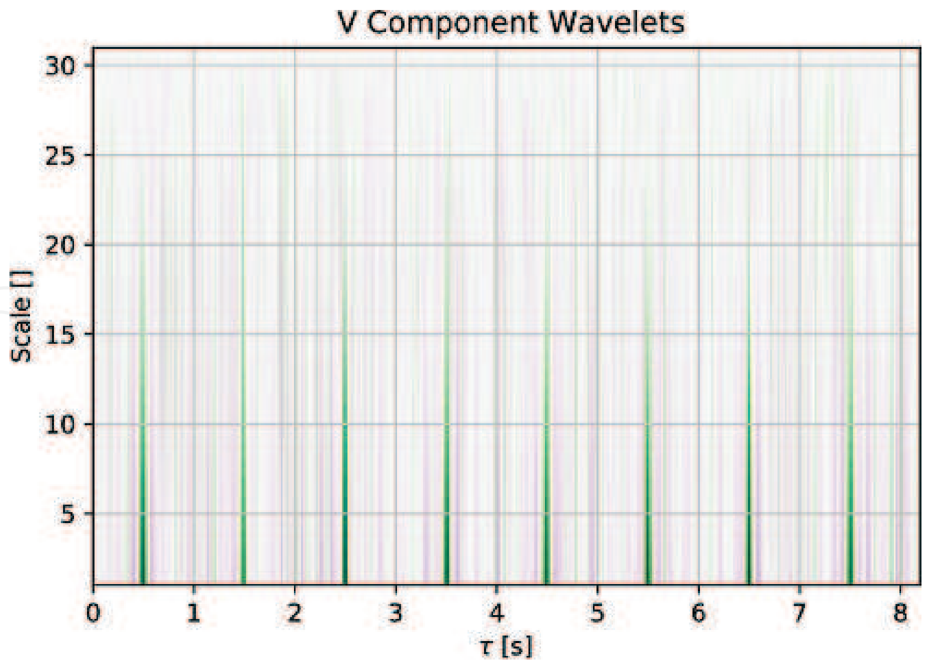

Figure 9. cwt on the V-component signal, with turbulent free flow.

The last technique to be presented here is how to detect a vortex passage when the turbulent velocity is higher than the vortex velocity. This is not always possible, but it can be done in some cases. The way to accomplish this is by taking more than one measurement synchronize with the vortex passage or with some phenomena that generate the vortex (this could be an oscillating surface, a pulsing jet, or the beginning of a movement that creates an steady state) and then take the mean of the measurements. By doing this, the turbulence present in the signals is going to be attenuated, and the periodic phenomenon present in all the signals is going to remain. After a wavelet transform can be used to detect the vortex passage, it must be said that if a complete synchronization is not achieved, a distortion may be present in the remaining signal, but if the difference in time is small compared to the time, it takes to the vortex to pass, the same results can be achieved.

Figures 10 and **11** show the results accomplished with the same simulation as in the case before but with a vortex velocity of 0.5% of the free flow velocity, using 15 different measurements.

It can be seen that, when the mean of different measurements the cwt shows the presence of the vortex.

This approach taken so far allows one to detect the presence of a vortex. To characterize it, there are many different techniques. Once the vortex is detected with the cwt, the maximum coefficient gives us the time (x axis) it passed and the scale (y axis) that it has respect to the wavelet scale. This scale is related to the time (or pseudo frequency) it took to the vortex to pass the point for further readings see [10]. The frequency shown in Ref. [10] relates to the time the vortex took to pass the anemometer as $1/f$, where f is the wavelet pseudo frequency, by knowing the mean velocity at the point the vortex size can be obtained with Eq. (3).

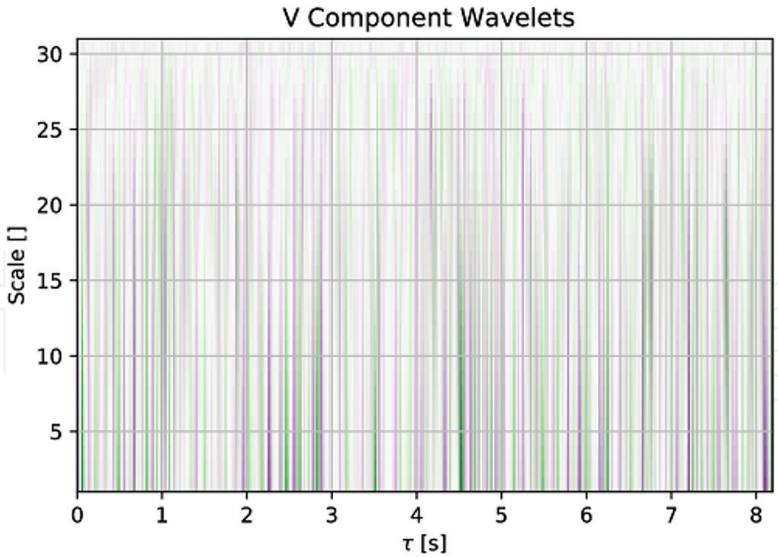

Figure 10. cwt on the V-component signal, with turbulent free flow, 1 measurement.

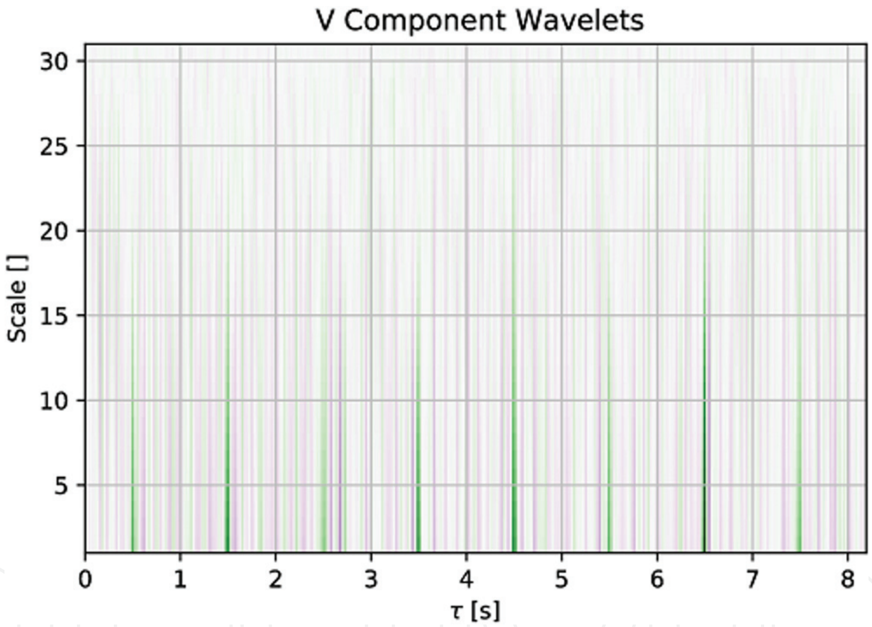

Figure 11. cwt on the V-component signal, with turbulent free flow, mean of 15 measurements.

$$S_v = V*t \tag{3}$$

S_v, is the vortex length or size, V is the point mean velocity, and t is the inverse of the pseudo frequency.

Each type of vortex would need a particular characterization, since it depends on the velocity distribution it has. For Rankine vortexes, the radius (or length) and the circulation Γ are sufficient. This last one is harder to obtain in the presence of a turbulent flow, but with a clean signal, different measurements points can be taken in height and relating the peak velocity of them to the velocity distribution in Eq. (1). For any other vortex, the velocity distribution must be known.

This is a helpful approach and gives one the tools in case the vortex has a known form. But in presence of multiple vortexes interacting with each other, this is not the best suited approach. For these kinds of flows, another parameters must be presented, such as representative scale.

To obtain a representative scale of the flow, the autocorrelation of the signal must be calculated first. This function is defined as in Eq. (4)

$$R(\tau) = \frac{\int u(t)*u(t-\tau)d\tau}{\int u(t)*u(t)dt} \tag{4}$$

As defined in Eq. (4), the autocorrelation function has a maximum value in $\tau = 0$ and is: $R(0) = 1$. This function is obviously discrete for measured signals and one only know the values for the sampled times. To define the representative scale, different criteria can be adopted, but most of them give similar results. Using them, one is able to obtain a representative scale of the smallest and the biggest vortex present in the flow, these are the microscale and macroscale, respectively. Here, three criteria are going to be introduced as presented in [11], one for the macroscale and two for the microscale. For the macroscale, the most commonly used criterion is the 0-passage. One interpretation for this criterion is that as long as the correlation does not become 0, the biggest vortex in the flow field is passing, once the vortex has passed, the autocorrelation function becomes 0. So, the 0-passage criteria would be as in Eq. (5).

$$\tau \textit{for the first } R(\tau) = 0 \tag{5}$$

After obtaining τ, one can use the same approach as with wavelets and define the macroscale of the vortex with Eq. (3).

For the microscale, the two criteria used are the “fist point slope,” and the $\mathbf{1}/\boldsymbol{e}$. This criteria are far less intuitive and require much reasoning and mathematical support. This exceeds the purpose of this chapter and there are not going to developed here, but for further reading see [6].

The first point slope criterion states that the microscale (scale in time) present in a turbulent flow, or in a flow with multiple vortexes interacting, is the time obtained by extrapolating a straight line that has the point (0,1) (first point of the autocorrelation function) and a slope equal to the slope of the autocorrelation function in its first point. This is as stated in Eq. (6).

$$\tau = -R(0)/R'(0) \tag{6}$$

As stated before, $\boldsymbol{R}(\mathbf{0})$ is the maximum value of $\boldsymbol{R}(\boldsymbol{\tau})$ so $\boldsymbol{R}'(\mathbf{0})$ must be negative, this gives a positive $\boldsymbol{\tau}$. As before, Eq. (3) can be used to compute the size of the vortex.

The last criterion is the $\mathbf{1}/\boldsymbol{e}$. This criterion simply states that the value of the time microscale is equal to the value $\boldsymbol{\tau}$ for which $\boldsymbol{R}(\boldsymbol{\tau})$=$\mathbf{1}/\boldsymbol{e}$ as in Eq. (7).

http://dx.doi.org/10.5772/intechopen.79504

$$\tau \textit{ for } R(\tau) = 1/e \tag{7}$$

This gives one a characterization of the spatial scales. Another useful approach is to determine the power spectrum density of the signal; this tells us how the energy is distributed in frequency. And can be useful in case a periodic phenomenon is present on the flow field.

The previous are the more classical techniques. But many more can be used. In general, to characterize any flow, one needs to have some knowledge of the phenomenon to capture. In the next section, other methods are going to be shown, for example, how an array of turfs can be useful to determine a longitudinal vortex diameter. Cross-correlation between spatial signals can help to determine if a certain flow structure is propagating or if it is been defused by turbulence, with an spatial anemometry array or PIV one can find the vortices field by taking the spatial derivatives of the velocities, and many for techniques are available, for further reading see [12].

3. Vortex generation

In the previous section, the main goal was to show how to characterize a passing vortex, this can be useful when a phenomenon is produced in an experiment and one needs to understand it, but vortex are always used for many different purposes in aerodynamics, one of the most simple approaches to passive flow control are vortex generators. These fixed surfaces are able to generate vortexes or stochastic turbulence in some cases. That is used to modify the behavior of a system. Also, when working with aerodynamic comfort for civil structures, or even to find the load in such structures, is always needed to test them inside a wind tunnel. In order to have a realistic view of the problem, the turbulence present in the atmospheric boundary layer must be modeled inside the wind tunnel. In these cases, one needs to generate vortex of certain scales, and to use the techniques presented before in order to determine if the turbulence generated fulfill the modeling criteria.

In this section, some useful techniques to generate vortexes of certain scales are presented, and what variables must be taken into account to accomplish a desired behavior.

The first method to be presented is the generation of a longitudinal vortex. This method is very effective, and allows the generation of a vortex with a well-defined diameter. A longitudinal vortex is a rotating structure along a define axis, this vortex has the particularity of changing its diameter along the axis. One common example of it is the wing tip vortex, present on any airplane, **Figure 12** shows an illustration of the phenomena.

The vortex shown in **Figure 12** is a result of the perturbation a wing generates downwards the flow, and it is a result of the tridimensionality of the wing. In practice, the presence of these kinds of vortexes result in a potential risk to an airplane, since their presence can drastically change the wing behavior. For those reasons, the study of such vortexes is highly important.

A way of generating these kinds of vortexes is by injecting compressed air at a certain incidence angle inside a tube. The resulting structure has a diameter in the order of the tube's

Figure 12. Longitudinal vortex representation.

Figure 13. Experimental set-up for longitudinal vortex generation.

diameter, and the velocities are a function of the pressure, flow rate, and incidence angle of the injected air. An experimental setup of such array is presented in **Figure 13**. Inside the tube, two hoses are connected with a fixed angle respect to the tube transversal plane: Pleasure and flow regulators are set between the tube and the air compressor to fix pressure and flow rate to a known value. The injection of air at a certain angle respect to the cylinders axis generates a rotary field, since the air must follow the surface of the cylinder, when this rotatory flow merges with the free flow entering the tube, a helical flow pattern is produced, and when the flow leaves the tube a helical vortex is generated, and then diffused as it moves in the flow

http://dx.doi.org/10.5772/intechopen.79504

direction. To characterize the vortex, a hot wire anemometer is set in front of the tube and spatial measurements of the velocity are taken, precisely the U-component and the V-component.

In this case, that the vortex has a well-defined diameter, a tufts array is handy to determine the diameter evolution along the axis, at different longitudinal positions downstream the vortex generator. This tufts array consists of a steel wire mesh with a 1 cm spacing, where thin threads of adequate color and a 4 cm length, to provide a good flow visualization, were fixed at each vertices of the mesh. The size of the turf array was about 44.5 cm height and 24 cm width. It can be seen in **Figure 14** how the tufts rotate and approximately define the vortex diameter.

In this setup, the tube diameter determines the size of the vortex, and a higher pressure and flow rate decreases the widening. A suitable characterization for these kinds of vortexes is the vortex size along the axis and the velocity distribution along the radius. **Figure 15** shows the vortex size evolution and **Figure 16** the velocity distribution.

The blue curve in **Figure 16** represents the U-component of the velocity and the red one the V-component for a tube with 6 cm diameter, 30 cm long and 45° of the flow entry. The rotational effect becomes clear by looking at the V-component, it evidenced by the change in the velocity sign. It is seen in **Figure 16** how velocity changes with the radius, and how it becomes 0 near the vortex size. This means that this are concentrated vortexes that rapidly disappear. As it is expected when the vortex moves, its diameter grows and the velocity diminish, this is a consequence of viscosity diffusion.

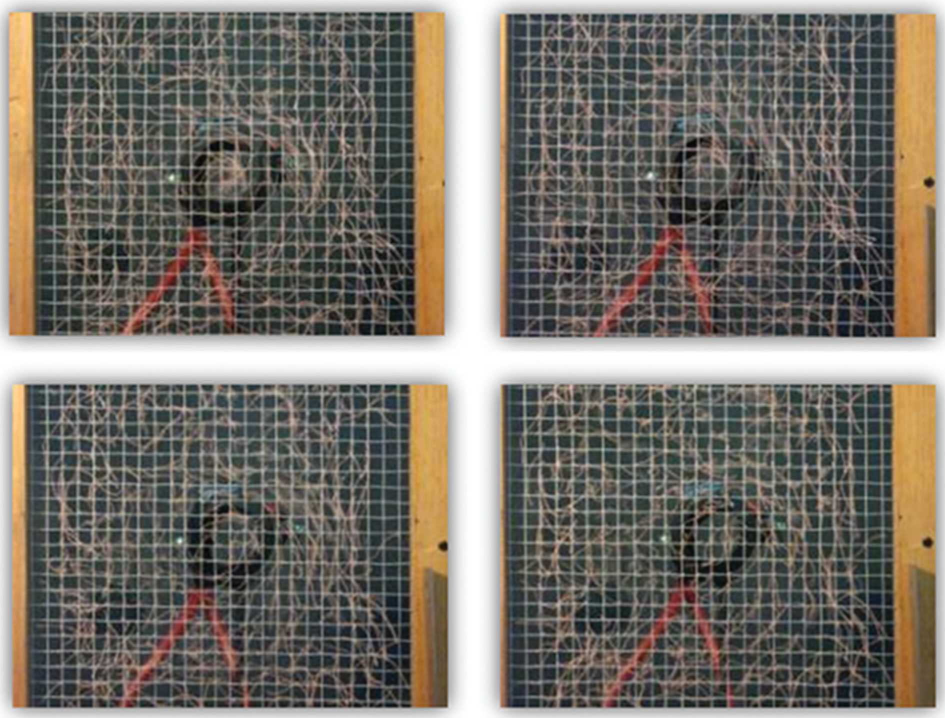

Figure 14. Visualization of the vortex diameter.

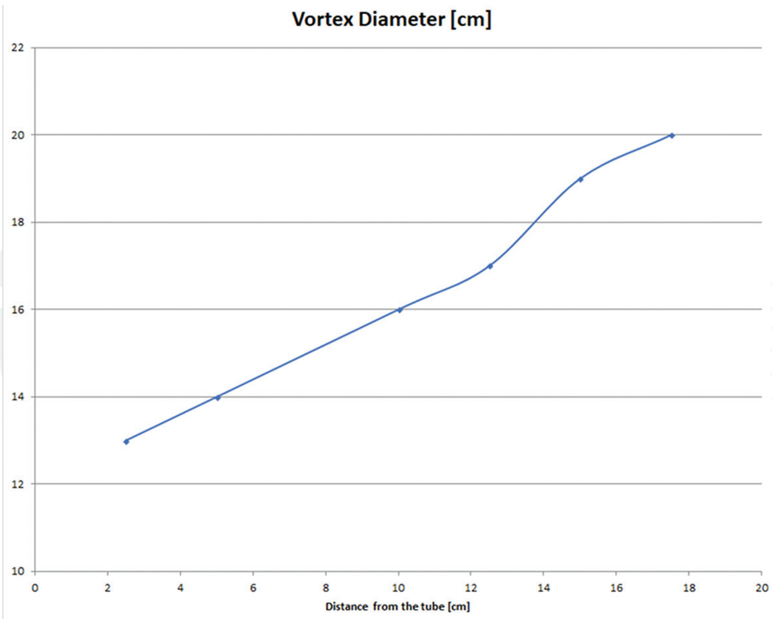

Figure 15. Vortex diameter for a 45° incidence and 4 bar pressure vs. distance from the vortex generator.

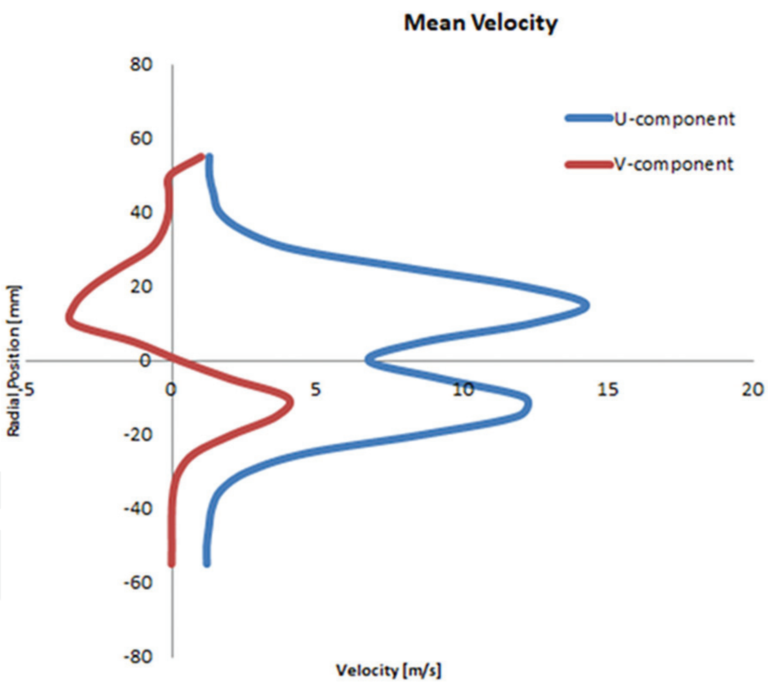

Figure 16. Velocity vs. radius. In red is the tangential component, in blue the axial component.

Another widely used method for generating vortex are fixed surface, in some cases called vortex generators (VG). This method is much simpler than the one presented before since it only requires a fixed surface. Almost any surface facing the flow will create vorticity or

Figure 17. Fin-type vortex generator, with a hot wire anemometer downwards.

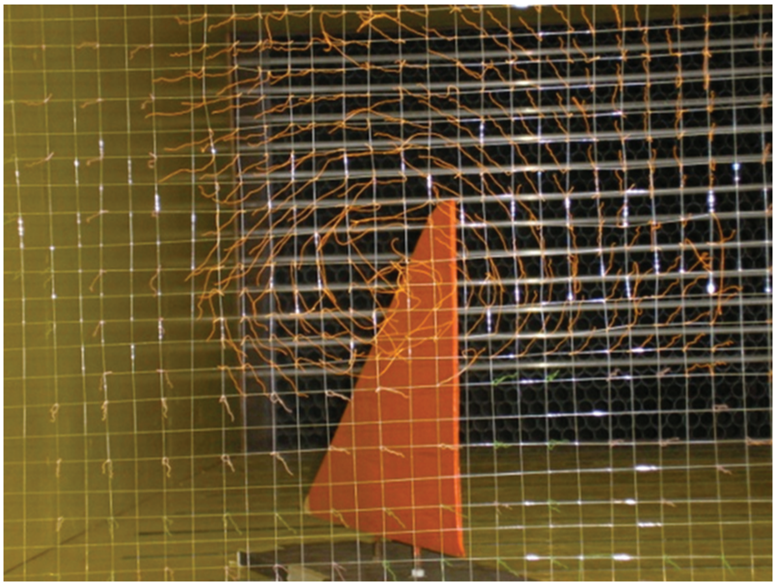

Figure 18. Fin-type vortex generator, producing a longitudinal vortex.

turbulence downwards itself. This method is usually used in airplane wings to delay the detachment of the boundary layer, this is possible by inserting energizes flow from the free flow to the boundary layer. **Figure 17** shows an example of them.

The main complexity with this method is that the generated vortex does not always have a defined structure. A delta wing or a fin, generates longitudinal vortex, but not in any Reynolds number or under any angle of attack. So the scales and the overall structure of the vortex can heavily depend among the flow condition. For this reason, these kind of devices are not usually characterized alone, but with the system they are meant to work with. **Figure 18** shows a longitudinal vortex generated by a fin VG, and a tufts array shown a helical vortex similar to the ones produced by a wing, the results of this experiment are going to be treated in the last section of the chapter.

When it is not possible to find a defined structure of the generated vortexes, the change in the scales, and turbulent intensity between the flow upstream the VG and downstream is a good way of quantify the VG behavior. Even if this approach does shows the full structure of the vortexes present in the flow, it allows one to estimate where the zone of influence is located; this is helpful to decide the separation of a VG array, for example, and allows one to know if the turbulence generated by one VG is going to interact with the one generated by its neighbor.

For fin-type VG, the main characteristic that will determine the turbulence intensity behind itself is the angle of attack or angle of attitude related to the flow. Increasing the angle of attack will increase the turbulence intensity behind itself, and will also increase the drag force over the VG, when vortex generation is the only concern, this is not a problem, but in applications like an airplane, this feature must be taken into account. More detailed information can be found in [13].

Figure 19 shows an experimental setup to determine the influence zone of a fin-type VG of 10 mm height and 25 mm long, positioned over a flat plate. In each of the planes, anemometric measurements were taken and the turbulence intensity present behind the VG was compared to the one of the free flow. For each, a point grid was generated to take the measurements, the planes shown are positioned at 12.5, 25, 50, and 100 mm, behind the VG. **Figure 20** shows the results of the turbulent intensity in the V-component, for the first and last plane shown in **Figure 19**, for a 6 m/s flow velocity, a 30° angle of incidence

It must be said that mean velocities in the point grid were analyzed too, but the results did not showed a coherent structure present in the flow field. But with the turbulence intensity field, one can see that the VG is able to change the overall structure of the flow. This property is extremely helpful when designing a flow control system, particularly a system whose intention is to trigger the turbulent transition of the boundary layer. The changes on the flow structure (as seen in **Figures 20** and **21**) are mostly held in the right side of the plane, this is due to the fact that the rotation of the VG (The 30° of incidence) left the tail positioned on the right side. The low pressure that forms in the back plane of the VG makes the flow to curl from the front plane to the back one, so it is expected that the velocities induced by the VG were stronger near the tail.

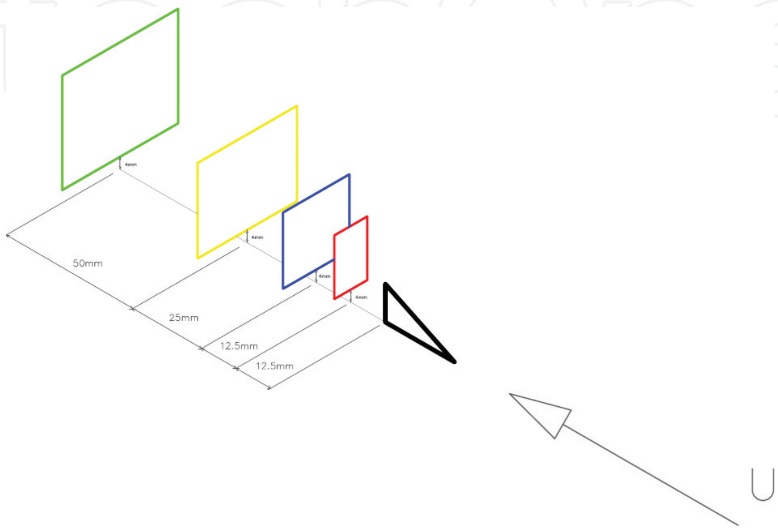

Figure 19. Grid planes for characterization of a fin-type vortex.

http://dx.doi.org/10.5772/intechopen.79504

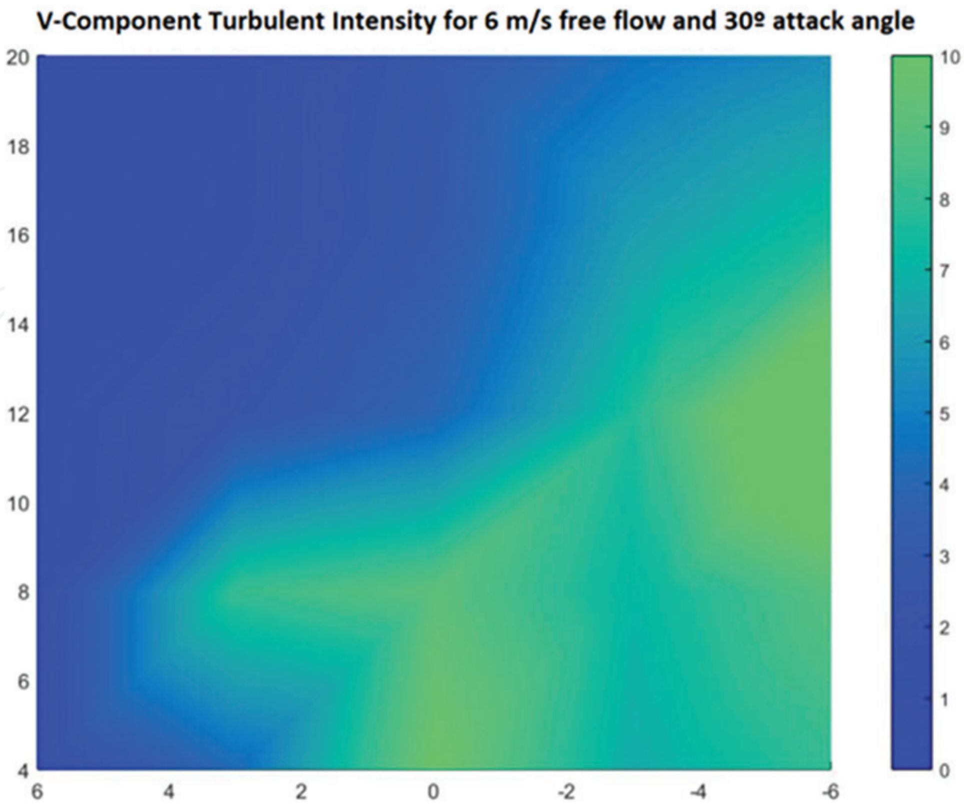

Figure 20. Turbulent intensity of the V-Component in the first plane, x and y axes are in mm, the VG is at position (0,0 in the plane).

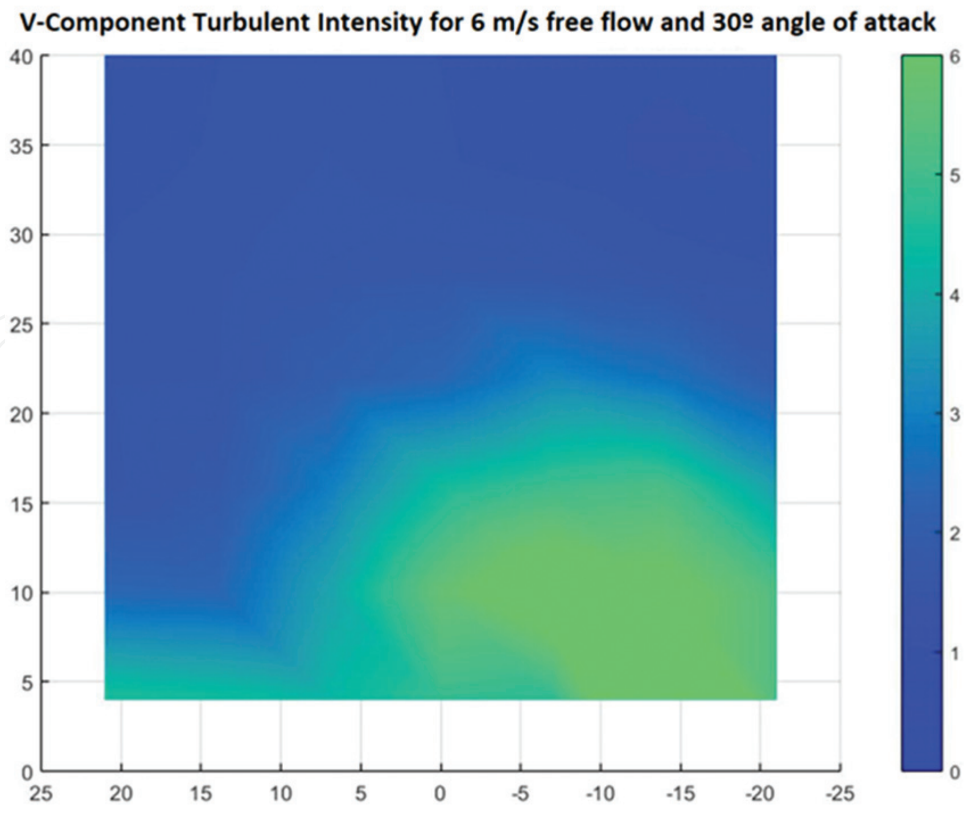

Figure 21. Turbulent intensity of the V-Component in the fourth plane, x and y axes are in mm, the VG is at position (0,0 in the plane).

4. Application example

This chapter shows how to detect, characterize, and generate vortexes; in order to give a full picture of their utility, in this last section, an application is shown. Vortexes are useful in flow control, needed to determine loads in civil structures, and can substantially change the behavior of a system when they are present in a free flow. To scratch the surface of this discipline, experimental results are presented here of the behavior of a wing in presence of a longitudinal vortex of a scale whit a size in the order of the wing chord. As it was mention before, longitudinal vortexes are produced by the wing tip of an airplane, so this approach can give us for example an insight of how an airplane it going to be affected in a formation flight.

The vortex in this experiment was generated by the fin VG presented in **Figure 18**. **Figure 22** shows a schematic of the experimental setup. For this experiment, a wing model was positioned in the wind tunnel test section, attached to force sensors, to determine the forces the wing produces. The model was placed between two end plates as shown in **Figure 22**, in order to minimize the 3D effects. Force measurements were taken and the Cl and Cd dimensionless coefficient determined. This experiment was repeated for different vortex configurations, which consisted of the same vortex positioned at different heights. One with the vortex center below the wing, one above, one at the same height of the wing chord, and one with no vortex (clean wing). As mentioned before, the vortex was generated with a VG, in this case, a coherent structure was produces, and its size was determined with a tufts array. Since the intention of this section is only to show how a system is modified when it is present in different vorticose structures, the full characterization of the vortex generated for this experiment is not relevant, and it is only going to be mentioned that the vortex size was similar to the wing chord.

Figures 23 and **24** show the C_l and the efficiently $E = C_l/C_d$ of the wing for the different configurations mentioned before.

Since no mass or momentum was added to generate the vortex here, the behavior of the wing in presence of the vortex, it is only a result of the coupling of the flow fields generated by both,

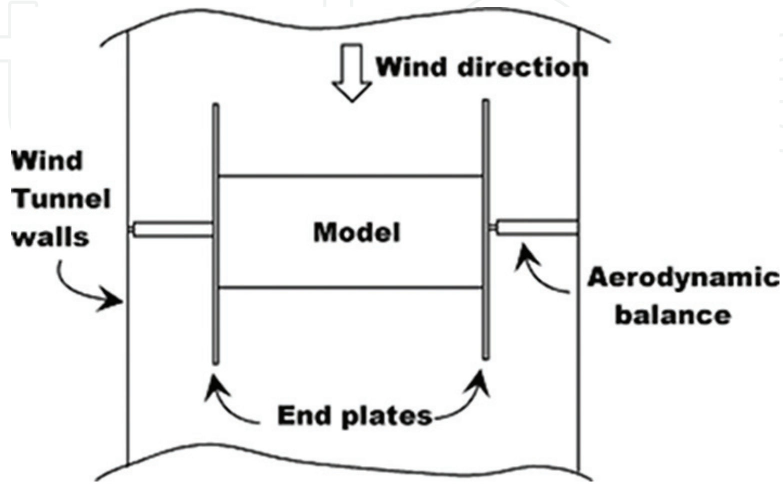

Figure 22. Experimental setup for the experiment, the fin is placed upwards the model.

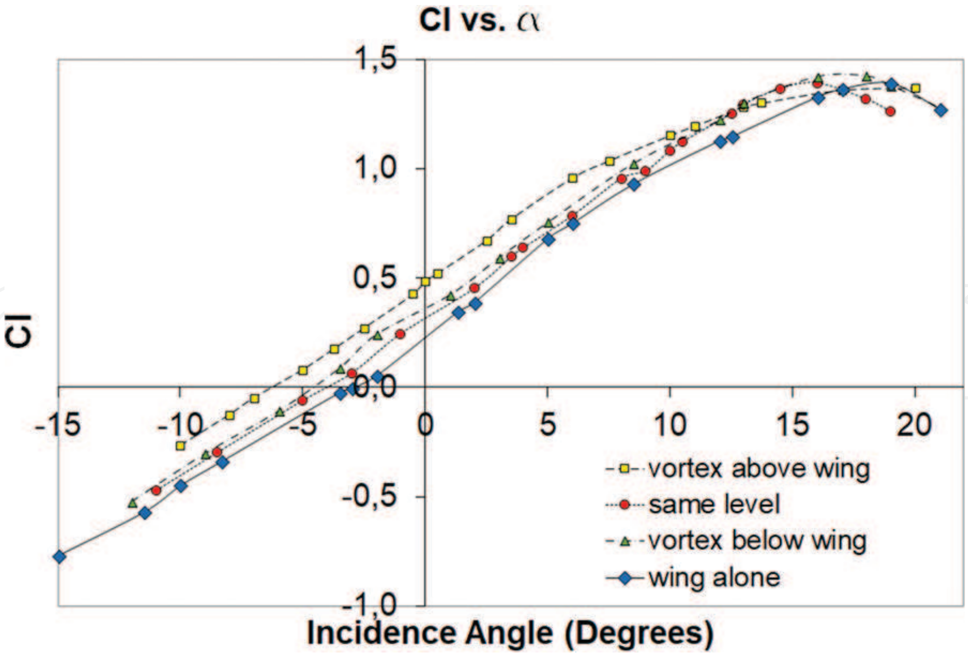

Figure 23. C_l coefficient for the wing in different conditions.

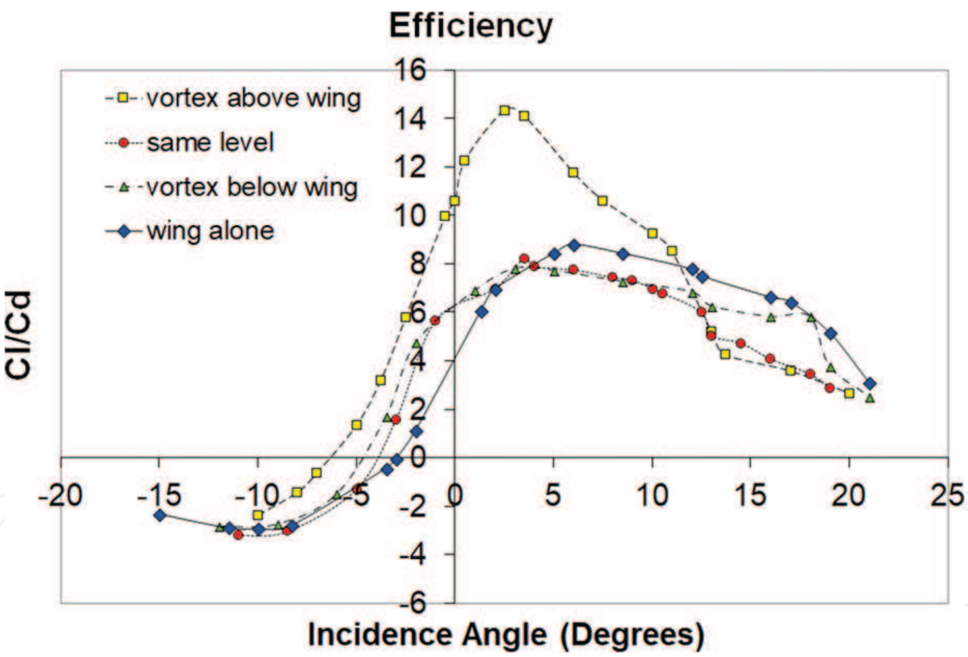

Figure 24. Efficiency of the wing in different conditions.

and not because of some extra energy present in the experiment. **Figure 24** shows clearly how a wing interacting with a vortex of its size can drastically change its performance. It is clear that the wing efficiency augments when the vortex is in the upper surface, but when the vortex is below the wing, not only the efficiency decreases, but also the stall occurs early. These kinds of result are expected since it is highly probable that the wing circulation become modified by the vorticity produced by the VG.

5. Conclusions

The main conclusions to be obtained from this work are the following:

1. As shown in Section 1, continuous wavelet transform can be used to detect a vortex passage in an anemometric measurement, even when the turbulence present in the flow has more energy than the vortex itself.
2. The characterization of any vortex is closely related to the vortex form, but some common characteristic can be obtain in any coherent structure such as radius (spatial scale) or velocity field, this can be done by detecting a passage in a time signal or by measuring the medium velocity field for longitudinal vortexes.
3. A vortex generator can modify the flow in different ways depending on the flow characteristics, as shown in the application part, a fin VG can generate a coherent structure, but for a different Reynolds number and in presence of a different geometry a fin-type VG may not generate a coherent structure, but the turbulent characteristics of the flow are always modified downstream the VG as is shown in the characterization section, and in this cases the definition of the macro and micro scales are useful.
4. It can be seen in this last experiment why the study of the vorticose structure in the free flow must be carried out, since it plays a main role in the behavior of a system, and can severely change the efficiency of such a system. Managing to characterize, generate and wisely use vortex can be helpful to modify the efficiency of a system to our will, and can be a highly beneficial approach.

Acknowledgements

We thank to bachelors Pablo Mantelli, Matias Jauregui Lorda and Gaston Santoiani for their collaboration with the measurements performed for this chapter.

Author details

Guillermo Martin Capittini[1,2]*, Julio Marañon Di Leo[1,2] and Juan Sebastian Delnero[1,2]

*Address all correspondence to: guillermo.capittini@ing.unlp.edu.ar

1 UIDET-LaCLyFA, Departamento Aeronáutica, Facultad de Ingeniería, Universidad Nacional de La Plata, La Plata, Buenos Aires, Argentina

2 CONICET, Ciudad de Buenos Aires, Argentina

References

[1] Williamson CHK, Roshko A. Vortex formation in the wake of an oscillating cylinder. Journal of Fluids and Structures. 1988;**2**(4):355-381. ISSN: 0889-9746

[2] Özgören M, Sahin B, Rockwell D. Vortex structure on a delta wing at high angle of attack. AIAA Journal. 2002;**40**(2):285-292

[3] Furman A, Breitsamter C. Turbulent and unsteady flow characteristics of delta wing vortex systems. Aerospace Science and Technology. 2013;**24**(1)

[4] Study on forms of vortex breakdown over delta wing. Chinese Journal of Aeronautics. 2004;**17**(1):17

[5] Graftieaux L, Michard M, Grosjean N. Combining PIV, POD and vortex identification algorithms for the study of unsteady turbulent swirling flows. Measurement Science and Technology. 2001;**12**:1422

[6] Alekseenko SV, Kuibin PA, Okulov VL. Theory of Concentrated Vortices, an Introduction. Springer; 2007. p. 134

[7] Kadambe S, Boudreaux-Bartels GF. Application of the wavelet transform for pitch detection. IEEE Transactions on Information Theory. 1992;**38**:917-934. Print ISNN: 00189448

[8] Mallat S, Hwang WL. Singularity detection and processing with wavelets. IEEE Transactions on information Theory. 1992;**38**:617-643. Print ISNN: 00189448

[9] Abbate A, Koay J, Frankel J, Schroeder SC, Das P. Application of wavelet transform signal processor to ultrasound. Ultrasonics Symposium IEEE 1994. 1994. Print ISBN: 0-78032012-3

[10] Matlab. [Internet]. Available from: https://www.mathworks.com/help/wavelet/ref/scal2frq.html

[11] Tropea C, Yarin C, Foss JH. Handbook of Experimental Fluid Dynamics. Springer; 2007. ISBN: 978-3-540-25141-5. Chapter 10

[12] Barlow JB, Rae WH, Pope A. Low Speed wind Tunnel Testing. 3rd ed. Wiley; 1999. ISBN: 0471-55774·9. Chapter 8

[13] Boldes U, Delnero JS, Colman J, Martinez MA, Marañón Di Leo J. Lift and drag behaviour of a low Reynolds wing section submitted to a nearby stream wise vortex. AIAA. 2008;**38**: 195-200